Angewandte
International Edition Chemie

Hydrogen Evolution

DOI: 10.1002/anie.201200082

Electrocatalytic and Photocatalytic Hydrogen Production in Aqueous Solution by a Molecular Cobalt Complex[**]

Wangkheimayum Marjit Singh, Teera Baine, Shotaro Kudo, Shiliang Tian, Xuan Anh N. Ma, Hongyu Zhou, Nathan J. DeYonker, Truc Chi Pham, John C. Bollinger, Daniel L. Baker, Bing Yan, Charles Edwin Webster, and Xuan Zhao**

Hydrogen as a source of clean and renewable fuel has attracted great interest because of its potential to reduce the current dependence on fossil fuels.[1] Reduction of water to H_2, especially with visible light, has been a subject of intense study and significant effort has been made to design metal complexes for proton reduction. Over the past few years, a considerable number of catalysts for H_2 evolution based on metal complexes such as Co,[2] Ni,[3] Fe,[4] and Mo[5] have been reported and extensively studied, especially in non-aqueous media, to provide insights into the mechanism of proton reduction. Recently, Eisenberg and co-workers described the photocatalytic proton reduction catalyzed by a mononuclear cobalt–dithiolene complex with a remarkable turnover number (TON) of >2700 per mol of Co catalyst in a 1:1 ratio of CH_3CN/H_2O.[2h] Although there has been significant progress in designing molecular catalysts for H_2 evolution, the search for robust and highly active catalysts that can operate in purely aqueous solution, by either electrochemical or photochemical approaches, still remains a great challenge.[2e,6]

Recently, molecular Co complexes supported by tetradentate or pentadentate ligands such as 2,6-bis(1,1-bis(2-pyridyl)ethyl)pyridine ($PY5Me_2$) have been reported to catalyze the reduction of protons in aqueous solution.[2e,7] We have designed a new type of pentadentate ligand, *N*,*N*-bis(2-pyridinylmethyl)-2,2′-bipyridine-6-methanamine (DPA-Bpy) and investigated the water oxidation activity of its Ru complex.[8] Here, we report the synthesis and characterization of a new type of mononuclear Co complex with the DPA-Bpy ligand that can serve as both electrocatalyst and photocatalyst for highly efficient production of H_2 in purely aqueous solution.

The reaction of $CoCl_2{\cdot}6H_2O$ with DPA-Bpy in CH_3CN heated at reflux results in a reddish cloudy solution. After filtration, the filtrate was dried under vacuum and washed with Et_2O to yield $Co(DPA\text{-}Bpy)Cl_2$ (**1**) as a light-pink powder (Scheme 1). The crystal structure of the Co^{III} form of **1** (see Figure S1 in the Supporting Information) confirmed that DPA-Bpy serves as a pentadentate ligand with a Co center in a distorted octahedral geometry with two *trans* pyridines groups, similar to that of $Ru(DPA\text{-}Bpy)Cl_3$.[8] The UV/Vis spectrum of **1** in water shows two intense bands at 247 and 300 nm from ligand $\pi \rightarrow \pi^*$ transitions, a shoulder peak at 337 nm, and a weak shoulder at 420 nm from a metal d–d transition (see Figure S2 in the Supporting Information). Heating an aqueous solution of **1** at reflux in the presence of $AgPF_6$ led to the formation of an aqua complex $[Co(DPA\text{-}Bpy)(OH_2)](PF_6)_3$ (**2**). Compared to **1**, complex **2** displays an absorption band at 470 nm originating from the metal d–d transition (see Figure S2 in the Supporting Information). The pK_a value of the coordinated H_2O in **2** was determined to be 5.0 by fitting the pH titration curve of **2** from pH 1 to 9 (Figure S3). The EPR spectrum of complex **1** showed a rhombic splitting pattern with *g* values of 5.56, 3.95, and 1.98, suggesting the presence of a high-spin Co^{II} center (Figure S4a).[9] The oxidation of **1** by $AgPF_6$ led to the formation of **2**, which showed an EPR-silent Co^{III} center (Figure S4b).

The cyclic voltammogram of complex **1** in CH_3CN displays three reversible redox potentials at 0.35, −0.94, and −1.53 V (vs. the standard hydrogen electrode, SHE), assignable to $Co^{III/II}$, $Co^{II/I}$, and $Co^{I/0}$, respectively (see Figure S5a and S5b in the Supporting Information). In the same region the ligand DPA-Bpy does not show any redox behavior (Figure S5c). In 1.0 M sodium phosphate buffer at pH 7.0, complex **2** exhibits a sequence of two redox events centered at 0.15 and −0.90 V (vs. SHE), corresponding to $Co^{III/II}$ and $Co^{II/I}$, respectively (Figure 1). The $Co^{III/II}$ couple displays a pH-dependent redox potential change, with a slope of −48 mV/pH in the range from pH 5 to 8 (Figure S6), suggesting a proton-coupled electron transfer process. How-

---

[*] Dr. W. M. Singh, T. Baine, S. Kudo, X. A. N. Ma, Dr. N. J. DeYonker, Dr. T. C. Pham, Prof. Dr. D. L. Baker, Prof. Dr. C. E. Webster, Prof. Dr. X. Zhao
Department of Chemistry, University of Memphis
Memphis, TN 38152 (USA)
E-mail: cewebstr@memphis.edu
xzhao1@memphis.edu

S. Tian, Dr. H. Zhou, Dr. J. C. Bollinger, Prof. Dr. B. Yan
Department of Chemical Biology & Therapeutics
St. Jude Children's Research Hospital
Memphis, TN, 38105-3678 (USA)

S. Tian
Department of Chemistry, University of Illinois
Urbana, IL 61801 (USA)

[**] We thank the Department of Chemistry at the University of Memphis, the University of Memphis High Performance Computing Facility and CROMIUM (Computational Research on Materials Institute at the University of Memphis) for support. We thank Derek Pegram for help with GC-TCD. We acknowledge support from the NSF, grant number EPS 1004083 (X.Z. and X.A.N.M.), the National Cancer Institute, grant number P30A027165 (B.Y.), and the American Lebanese Syrian Associated Charities (ALSAC) (B.Y.). We also thank Dr. Yi Lu from the University of Illinois for help with the EPR measurements.

Supporting information for this article is available on the WWW under http://dx.doi.org/10.1002/anie.201200082.

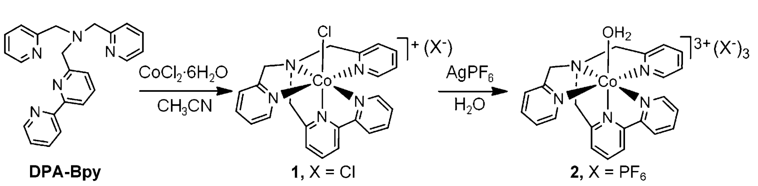

Scheme 1. Synthesis of **1** and **2**.

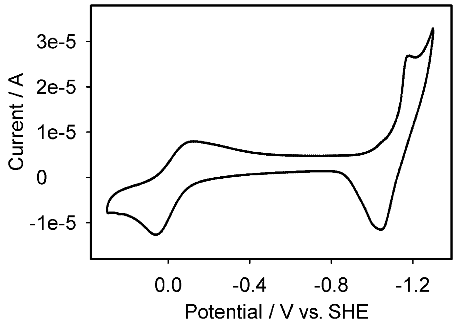

Figure 1. Cyclic voltammogram of **2** in 1.0 M sodium phosphate buffer at pH 7.0. Scan rate, 100 $mV s^{-1}$. Working electrode, glassy carbon; reference electrode, Ag/AgCl; counter electrode, Pt wire.

ever, the $Co^{III/II}$ couple only changes slightly within the range from pH 1 to 5. The Pourbaix diagram of **2** is consistent with a pK_a of 5.0 for the Co^{III}–OH_2 species, as obtained from pH titration of **2**.

When a mercury pool was used as the working electrode, the cyclic voltammogram of 1.0 M sodium phosphate buffer at pH 7 showed no significant current at potentials more positive than −1.6 V vs. SHE (see Figure S7 in the Supporting Information). However, in the presence of complex **2**, a strong current appeared at −1.20 V vs. SHE concomitant with the formation of gas bubbles, which was confirmed to be H_2 by GC-TCD analysis (GC = gas chromatography, TCD = thermal conductivity detector). This study suggested that **2** is capable of catalyzing the reduction of protons from neutral water to H_2. To determine the overpotential for the proton reduction by **2**, we have carried out control potential experiments using an H-type electrochemical cell. Figure S8 displays the charge build-up during the electrolysis over 200 s at varied potentials for 50 μM **2** in 1.0 M phosphate buffer at pH 7. There is no significant charge consumption for overpotentials below −0.55 V, and the catalytic current for the proton reduction occurs at an overpotential of −0.60 V (−1.01 V vs. SHE), close to the $Co^{II/I}$ couple at −0.90 V (vs. SHE).

To evaluate the current efficiency of H_2 production, bulk electrolysis of 1.0 M phosphate buffer at pH 7 was carried out in the presence of **2** under room temperature at a potential of −1.4 V (vs. SHE). The evolved H_2 was confirmed by GC-TCD and quantified volumetrically by a gas burette. For **2** in the range of 50 μM–1 mM, we obtained a current efficiency of $(99 \pm 1)\,\%$ (see Table S1 in the Supporting Information) for the evolution of H_2 at pH 7 (Table S1). When the controlled potential experiment was conducted at −1.3 V (vs. SHE), the Faradaic efficiency was determined to be $(98 \pm 2)\,\%$. On the basis of consumed charges over 1 h of bulk electrolysis at −1.4 V (vs. SHE) in 1.0 M phosphate buffer at pH 7 in the presence of 50 μM **2**, the activity for the H_2 evolution of **2** was calculated to be $1400\ L\,H_2\,(mol\,cat)^{-1}\,h^{-1}\,(cm^2\,Hg)^{-1}$ (Figure S9a), or a turnover number (TON) of $> 300\ mol\,H_2\,(mol\,cat)^{-1}$, suggesting that the reduced form of complex **2** is a highly efficient electrocatalyst for proton reduction in neutral aqueous solution. However, as shown in Figure S9b, the activity of **2** decreased rapidly after more than 3 h of electrolysis.

Photocatalytic H_2 evolution based on Co catalysts has been a subject of intense research over the past few years.[2g,6b–d,g,10] We have investigated photocatalytic H_2 production by complex **2** using ascorbic acid as electron donor and $[Ru(bpy)_3]^{2+}$ as photosensitizer. Previous studies on photocatalytic systems using ascorbic acid and $[Ru(bpy)_3]^{2+}$ have shown a pH-dependent activity for H_2 evolution with catalysts being most active at pH 4.0.[2h,4h]

We carried out photolysis experiments in 10 mL of 1.0 M acetate buffer solution at pH 4.0 containing 0.1 M ascorbic acid and 0.5 mM $[Ru(bpy)_3]^{2+}$. As shown in Figure 2 and Figure S10a, formation of H_2 was observed upon photolysis (light of a light emitting diode, LED, at 450 nm) of the above pH 4 solution in the presence of 5.0 μM **2**. The H_2 evolution process ceased in around 3 h, with a TON of $> 1600\ mol\,H_2\,(mol\,cat)^{-1}$. However, nearly 90 % of the H_2 evolved within the first hour of irradiation, corresponding to a turnover frequency (TOF) of $1500\ mol\,H_2\,(mol\,cat)^{-1}\,h^{-1}$ (Figure 2). To determine the pH effects on H_2 evolution catalyzed by **2**, light-induced H_2 evolution was performed in the pH range of 3–6 under the conditions described in Figure 2. We observed an optimum pH of 4.0 for the evolution of H_2, the same as those of previously reported systems (see Figure S11 in the Supporting Information).[2h,4h] Such pH-dependent activity has been related to the pK_a of ascorbic acid because ascorbic acid acts as both a proton and electron donor for the production of H_2.[4h] Control experiments without ascorbic acid, $[Ru(bpy)_3]^{2+}$, or **2** showed no or only residual amounts of H_2 production, suggesting all three components are required for the evolution of H_2 (Figure S10b).

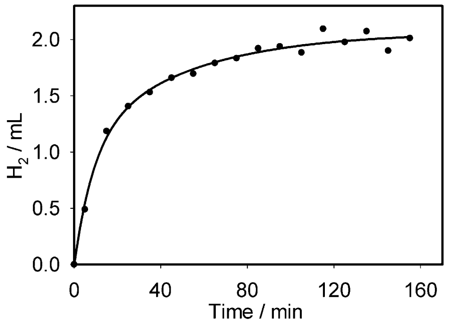

Figure 2. Photocatalytic H_2 production over time in 1.0 M acetate buffer at pH 4.0 with 0.1 M ascorbic acid, 0.5 mM $[Ru(bpy)_3]^{2+}$, and 5.0 μM **2** at 22 °C.

To explore the dependence of the H_2 activity on the concentration of **2**, we conducted photolysis experiments under different concentration of **2** (0.5–50 μM) at pH 4.0. As shown in Figure S12 in the Supporting Information, the concentration of **2** has a great influence on the light-induced activity for H_2 evolution in terms of TON and TOF, which increased significantly at lower concentration of the catalyst. At 50 μM **2**, we obtained a TON of around 450 mol H_2 (mol cat)$^{-1}$ and a TOF of 410 mol H_2 (mol cat)$^{-1}$ h^{-1}. However, at 0.5 μM **2**, the TON and TOF increased drastically to 4400 mol H_2 (mol cat)$^{-1}$ and 4000 mol H_2 (mol cat)$^{-1}$ h^{-1}, respectively. The dependence of TON and TOF on the catalyst concentration indicates that the formation of binuclear or polynuclear species might be involved in the inactivation of complex **2**.

The light-induced H_2 production catalyzed by **2** also depends on the concentrations of sacrificial reagent and photosensitizer. When a photolysis experiment was conducted at higher concentration of ascorbic acid (0.5 M) and $[Ru(bpy)_3]^{2+}$ (2.0 mM) with 5.0 μM **2**, the TON increased further from 1600 to 2100 mol H_2 (mol cat)$^{-1}$, corresponding to a TOF of > 1900 mol H_2 (mol cat)$^{-1}$ h^{-1} during the first hour of irradiation (see Figure S13 in the Supporting Information). Therefore, our studies demonstrated that the reduced form of complex **2** acts as a highly efficient photocatalyst for the evolution of H_2.

To identify factors responsible for the decomposition of the photocatalytic H_2 evolution in the above system, we added one of the three components (ascorbic acid, $[Ru(bpy)_3]^{2+}$, or complex **2**) to a reaction flask after cessation of the H_2 evolution to see if the H_2 production could be resumed. However, addition of any of the three components, in the same amount as used in the photocatalytic reaction, resulted in no significant amount of H_2 formation, suggesting that decomposition of all three species occurred during the photocatalytic H_2 evolution. Both complex **2** and the photosensitizer need to be added to resume the production of H_2, with around 37 % more production of H_2 (see Figure S14 in the Supporting Information). The addition of both ascorbic acid and $[Ru(bpy)_3]^{2+}$ also led to an increase in H_2 evolution by around 10 %. However, no significant amount of H_2 was produced when both ascorbic acid and complex **2** were added, suggesting a complete decomposition of $[Ru(bpy)_3]^{2+}$ under our reaction conditions. The coordination of an acetate ion to catalyst **2** or the substitution of the bpy ligand in $[Ru(bpy)_3]^{2+}$ by an acetate ion may contribute to the decomposition of the photocatalytic system for H_2 evolution. Furthermore, the presence of a trace amount of air in the reaction flask may also lead to the decomposition of the catalytic system. The amount of H_2 produced in the presence of air is only 40 % of that produced when the H_2 evolution was conducted in Ar, suggesting that O_2 inhibits the evolution of H_2.

The catalytic H_2 production at a potential lower than the $Co^{II/I}$ couple of **2** suggested that the Co^I form of **2** may be responsible for the proton reduction. A number of possible mechanisms, involving mononuclear or binuclear pathways, have been proposed to account for the evolution of H_2 catalyzed by molecular Co complexes.[2i,11] Both homolytic and heterolytic mechanisms may work simultaneously for a system depending on particular reaction conditions.[12] To provide insight into the mechanism of proton reduction by **2**, we performed DFT calculations to explore the possible reaction intermediates, and the reaction free-energy changes of possible pathways for the proton reduction (see Table S3, Schemes S1 and S2, and Figure S14 in the Supporting Information).[11] Results from DFT computations suggest that a number of reaction pathways are thermodynamically favorable for the proton reduction by **2**, such as the one shown in Scheme 2 where the binding of the proton to the Co^I form of **2** yields the Co^{III}–H species. Further reduction of the Co^{III}–H to the Co^{II}–H species followed by binding of another proton results in the evolution of H_2 (Scheme 2).[11]

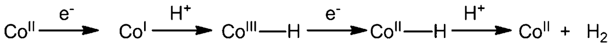

Scheme 2. Proposed mechanism for the proton reduction by **2**.

Photocatalytic H_2 production in systems using ascorbic acid as electron donor and $[Ru(bpy)_3]^{2+}$ as photosensitizer have been reported.[2g,i] Previous studies have shown that reductive quenching of the excited state of $[Ru(bpy)_3]^{2+}$ by ascorbic acid could lead to the formation of $[Ru(bpy)_3]^{+}$, which can reduce Co^{II} to Co^I before proton binding and reduction.[2h,6j,13] Kinetic and mechanistic studies are underway to identify the exact mechanisms for H_2 evolution catalyzed by **2**.

In summary, we have presented a new type of mononuclear Co complex with pentadentate ligand that can highly efficiently catalyze the production of H_2 in purely aqueous solution by both electrochemical and photochemical approaches. The modification of the ligand scaffolds to further tune the redox properties and activity for the H_2 evolution by **2** is currently in progress.

Experimental Section

All experiments were conducted in an Ar atmosphere unless noted otherwise. The detailed synthesis of $Co(DPA\text{-}Bpy)Cl_2$ (**1**) and $[Co(DPA\text{-}Bpy)(OH_2)](PF_6)_3$ (**2**) are described in the Supporting Information. Controlled potential electrolysis was conducted in 1.0 M sodium phosphate buffer at pH 7 in an H-type gas-tight dual compartment cell. A mercury pool with a surface area of 4.9 cm^2 was used as working electrode that was connected through a platinum wire placed at the bottom of the mercury pool. The solution was stirred constantly during the electrolysis experiments at controlled potentials. A platinum gauze wire, used as auxiliary electrode, was placed in the other compartment separated from the solution of the working electrode. An aqueous Ag/AgCl electrode was used as the reference electrode. The working and auxiliary compartments both contained 22.5 mL of electrolyte solution, which were thoroughly degassed by purging with Ar for 30 min prior to the experiments. The Faradaic efficiency was determined with 50 μM **2** at an applied potential of −1.3 and −1.4 V vs. SHE. The experiments were performed at 22 °C and the vapor pressure of water at 22 °C (19.8 mmHg) was corrected by calculating the current efficiency of H_2 production.

For the photocatalytic H_2 evolution, each sample was prepared in a 130 mL rectangular flask containing 10 mL of buffer in the presence of $[Ru(bpy)_3]Cl_2$, ascorbic acid, and complex **2**. The flask was sealed with a septum, degassed under vacuum, and flushed with Ar (with 5 %

CH_4) four times to remove any air present. Each sample was irradiated by LED light (450 nm) at room temperature under constant stirring. The amounts of H_2 produced during electrolysis or photocatalysis were determined by gas chromatography using a HP 5890 series II gas chromatograph with a TCD detector (5 Å molecular sieve column) or measured volumetrically by a gas burette.

Received: January 4, 2012
Revised: April 4, 2012

Keywords: cobalt · electrocatalysis · homogeneous catalysis · hydrogen · photochemistry

---

[1] a) N. S. Lewis, D. G. Nocera, *Proc. Natl. Acad. Sci. USA* **2006**, *103*, 15729–15735; b) V. Balzani, A. Credi, M. Venturi, *ChemSusChem* **2008**, *1*, 26–58; c) J. Barber, *Biochem. Soc. Trans.* **2006**, *34*, 619–631; d) O. Kruse, J. Rupprecht, J. H. Mussgnug, G. C. Dismukes, B. Hankamer, *Photochem. Photobiol. Sci.* **2005**, *4*, 957–970.

[2] a) P. V. Bernhardt, L. A. Jones, *Inorg. Chem.* **1999**, *38*, 5086–5090; b) X. Hu, B. S. Brunschwig, J. C. Peters, *J. Am. Chem. Soc.* **2007**, *129*, 8988–8998; c) C. Baffert, V. Artero, M. Fontecave, *Inorg. Chem.* **2007**, *46*, 1817–1824; d) J. P. Bigi, T. E. Hanna, W. H. Harman, A. Chang, C. J. Chang, *Chem. Commun.* **2010**, *46*, 958–960; e) Y. Sun, J. P. Bigi, N. A. Piro, M. L. Tang, J. R. Long, C. J. Chang, *J. Am. Chem. Soc.* **2011**, *133*, 9212–9215; f) P.-A. Jacques, V. Artero, J. Pécaut, M. Fontecave, *Proc. Natl. Acad. Sci. USA* **2009**, *106*, 20627–20632; g) J. L. Dempsey, B. S. Brunschwig, J. R. Winkler, H. B. Gray, *Acc. Chem. Res.* **2009**, *42*, 1995–2004; h) W. R. McNamara, Z. Han, P. J. Alperin, W. W. Brennessel, P. L. Holland, R. Eisenberg, *J. Am. Chem. Soc.* **2011**, *133*, 15368–15371; i) V. Artero, M. Chavarot-Kerlidou, M. Fontecave, *Angew. Chem.* **2011**, *123*, 7376–7405; *Angew. Chem. Int. Ed.* **2011**, *50*, 7238–7266; j) R. M. Kellett, T. G. Spiro, *Inorg. Chem.* **1985**, *24*, 2373–2377; k) G. M. Jacobsen, J. Y. Yang, B. Twamley, A. D. Wilson, R. M. Bullock, M. Rakowski DuBois, D. L. DuBois, *Energy Environ. Sci.* **2008**, *1*, 167–174; l) E. S. Wiedner, J. Y. Yang, W. G. Dougherty, W. S. Kassel, R. M. Bullock, M. R. DuBois, D. L. DuBois, *Organometallics* **2010**, *29*, 5390–5401; m) C. Creutz, N. Sutin, *Coord. Chem. Rev.* **1985**, *64*, 321–341; n) N. Sutin, C. Creutz, E. Fujita, *Comments Inorg. Chem.* **1997**, *19*, 67–92.

[3] a) J. P. Collin, A. Jouaiti, J. P. Sauvage, *Inorg. Chem.* **1988**, *27*, 1986–1990; b) M. Rakowski Dubois, D. L. Dubois, *Acc. Chem. Res.* **2009**, *42*, 1974–1982; c) A. Le Goff, V. Artero, B. Jousselme, P. D. Tran, N. Guillet, R. Métayé, A. Fihri, S. Palacin, M. Fontecave, *Science* **2009**, *326*, 1384–1387; d) U. J. Kilgore, J. A. S. Roberts, D. H. Pool, A. M. Appel, M. P. Stewart, M. R. DuBois, W. G. Dougherty, W. S. Kassel, R. M. Bullock, D. L. DuBois, *J. Am. Chem. Soc.* **2011**, *133*, 5861–5872; e) M. L. Helm, M. P. Stewart, R. M. Bullock, M. R. DuBois, D. L. DuBois, *Science* **2011**, *333*, 863–866.

[4] a) G. A. N. Felton, A. K. Vannucci, J. Chen, L. T. Lockett, N. Okumura, B. J. Petro, U. I. Zakai, D. H. Evans, R. S. Glass, D. L. Lichtenberger, *J. Am. Chem. Soc.* **2007**, *129*, 12521–12530; b) M. Y. Darensbourg, E. J. Lyon, X. Zhao, I. P. Georgakaki, *Proc. Natl. Acad. Sci. USA* **2003**, *100*, 3683–3688; c) C. Tard, X. Liu, S. K. Ibrahim, M. Bruschi, L. D. Gioia, S. C. Davies, X. Yang, L.-S. Wang, G. Sawers, C. J. Pickett, *Nature* **2005**, *433*, 610–613; d) L. Sun, B. Åkermark, S. Ott, *Coord. Chem. Rev.* **2005**, *249*, 1653–1663; e) S. Kaur-Ghumaan, L. Schwartz, R. Lomoth, M. Stein, S. Ott, *Angew. Chem.* **2010**, *122*, 8207–8211; *Angew. Chem. Int. Ed.* **2010**, *49*, 8033–8036; f) R. Mejia-Rodriguez, D. Chong, J. H. Reibenspies, M. P. Soriaga, M. Y. Darensbourg, *J. Am. Chem. Soc.* **2004**, *126*, 12004–12014; g) F. Gloaguen, J. D. Lawrence, T. B. Rauchfuss, *J. Am. Chem. Soc.* **2001**, *123*, 9476–9477; h) F. Wang, W.-G. Wang, X.-J. Wang, H.-Y. Wang, C.-H. Tung, L.-Z. Wu, *Angew. Chem.* **2011**, *123*, 3251–3255; *Angew. Chem. Int. Ed.* **2011**, *50*, 3193–3197; i) P. Poddutoori, D. T. Co, A. P. S. Samuel, C. H. Kim, M. T. Vagnini, M. R. Wasielewski, *Energy Environ. Sci.* **2011**, *4*, 2441–2450; j) W. M. Singh, D. Pegram, H. Duan, D. Kalita, P. Simone, G. L. Emmert, X. Zhao, *Angew. Chem.* **2012**, *124*, 1685–1688; *Angew. Chem. Int. Ed.* **2012**, *51*, 1653–1656.

[5] a) A. M. Appel, D. L. DuBois, M. R. DuBois, *J. Am. Chem. Soc.* **2005**, *127*, 12717–12726; b) H. I. Karunadasa, C. J. Chang, J. R. Long, *Nature* **2010**, *464*, 1329–1333.

[6] a) H. Ozawa, M. Haga, K. Sakai, *J. Am. Chem. Soc.* **2006**, *128*, 4926–4927; b) T. Lazarides, T. McCormick, P. Du, G. Luo, B. Lindley, R. Eisenberg, *J. Am. Chem. Soc.* **2009**, *131*, 9192–9194; c) P. Zhang, M. Wang, J. Dong, X. Li, F. Wang, L. Wu, L. Sun, *J. Phys. Chem. C* **2010**, *114*, 15868–15874; d) A. Fihri, V. Artero, M. Razavet, C. Baffert, W. Leibl, M. Fontecave, *Angew. Chem.* **2008**, *120*, 574–577; *Angew. Chem. Int. Ed.* **2008**, *47*, 564–567; e) D. Streich, Y. Astuti, M. Orlandi, L. Schwartz, R. Lomoth, L. Hammarström, S. Ott, *Chem. Eur. J.* **2010**, *16*, 60–63; f) J. L. Dempsey, J. R. Winkler, H. B. Gray, *J. Am. Chem. Soc.* **2010**, *132*, 1060–1065; g) T. M. McCormick, B. D. Calitree, A. Orchard, N. D. Kraut, F. V. Bright, M. R. Detty, R. Eisenberg, *J. Am. Chem. Soc.* **2010**, *132*, 15480–15483; h) B. Probst, A. Rodenberg, M. Guttentag, P. Hamm, R. Alberto, *Inorg. Chem.* **2010**, *49*, 6453–6460; i) F. Gärtner, B. Sundararaju, A.-E. Surkus, A. Boddien, B. Loges, H. Junge, P. H. Dixneuf, M. Beller, *Angew. Chem.* **2009**, *121*, 10147–10150; *Angew. Chem. Int. Ed.* **2009**, *48*, 9962–9965; j) C. V. Krishnan, N. Sutin, *J. Am. Chem. Soc.* **1981**, *103*, 2141–2142.

[7] B. D. Stubbert, J. C. Peters, H. B. Gray, *J. Am. Chem. Soc.* **2011**, *133*, 18070–18073.

[8] B. Radaram, J. A. Ivie, R. M. Grudzien, J. H. Reibenspies, C. E. Webster, X. Zhao, *Inorg. Chem.* **2011**, *50*, 10564–10571.

[9] A. Bencini, C. Benelli, D. Gatteschi, C. Zanchini, *Inorg. Chem.* **1980**, *19*, 3027–3030.

[10] a) B. Probst, C. Kolano, P. Hamm, R. Alberto, *Inorg. Chem.* **2009**, *48*, 1836–1843; b) K. L. Mulfort, D. M. Tiede, *J. Phys. Chem. B* **2010**, *114*, 14572–14581.

[11] a) B. H. Solis, S. Hammes-Schiffer, *Inorg. Chem.* **2011**, *50*, 11252–11262; b) B. H. Solis, S. Hammes-Schiffer, *J. Am. Chem. Soc.* **2011**, *133*, 19036–19039.

[12] U. Koelle, S. Paul, *Inorg. Chem.* **1986**, *25*, 2689–2694.

[13] a) C. Creutz, N. Sutin, B. S. Brunschwig, *J. Am. Chem. Soc.* **1979**, *101*, 1297–1298; b) J. L. Dempsey, J. R. Winkler, H. B. Gray, *J. Am. Chem. Soc.* **2010**, *132*, 16774–16776.